Noncoherent Ultra-Wideband (De)Modulation

Liuqing Yang, *Senior Member, IEEE*, Georgios B. Giannakis, *Fellow, IEEE*, and Ananthram Swami, *Senior Member, IEEE*

***Abstract*—Ultra-wideband (UWB) radios have received increasing attention recently for their potential to overlay legacy systems, their low-power consumption and low-complexity implementation. Because of the pulsed or duty-cycled nature of the ultra-short transmitted waveforms, timing synchronization and channel estimation pose major, and often conflicting, challenges and requirements. In order to address (or in fact bypass) both tasks, we design and test noncoherent UWB (de)modulation schemes, which remain operational even without timing and channel information. Relying on integrate-and-dump operations of what we term "dirty templates," we first derive a maximum likelihood (ML) optimal noncoherent UWB demodulator. We further establish a conditional ML demodulator with lower complexity. Analysis and simulations show that both can also be applied after (possibly imperfect) timing acquisition. Under the assumption of perfect timing, our noncoherent UWB scheme reduces to a differential UWB system. Our approach can also be adapted to a transmitted reference (TR) UWB system. We show that the resultant robust-to-timing TR (RTTR) approach considerably improves performance of the original TR system in the presence of timing offsets or residual timing acquisition errors.**

***Index Terms*—Channel estimation, differential modulation, noncoherent detection, timing synchronization, transmitted reference (TR), ultra-wideband (UWB).**

I. Introduction

THE growing interest in ultra-wideband (UWB) radios stems from their attractive features which include low probability of detection (LPD), low-power and low-complexity baseband operation, and potentially high data rates. These make UWB connectivity suitable for indoor and especially short-range high-rate wireless links in the workplace and at home, as well as for tactical outdoor communications.

Timing synchronization (a.k.a. timing offset estimation) and channel estimation pose two formidable challenges in enabling the unique benefits of UWB transmissions and constitute two major hurdles towards achieving capacity in the UWB regime [14]. Timing synchronization algorithms have been developed to provide reasonable performance even when the multipath channel is *unknown* [22]. However, residual timing errors are inevitable, especially under low complexity constraints. On the other hand, modulation schemes exist that do not require explicit receiver-side channel estimation. These include the transmitted reference (TR) algorithm which correlates each received information-bearing waveform with an accompanying pilot waveform [11], [12]; and the differential scheme which demodulates by correlating adjacent received information waveforms [9], [10]. Optimized versions of TR are also available that recover most of its 50% rate or energy loss [23], [24]. Although TR relaxes timing requirements, its operation and performance heavily depend on timing synchronization.

In this paper, we develop and test a *noncoherent* demodulation algorithm, which remains operational even when timing and channel estimation are both bypassed. Our scheme builds on the correlation between neighboring "dirty" templates—a tool used in [22] for timing synchronization without channel knowledge. Different from these timing algorithms, our technique here enables demodulation *without* timing and channel knowledge. Similar to TR and differential schemes, our demodulation algorithm avoids channel estimation by cross-correlating adjacent segments of the noisy received waveform and enjoys low-complexity implementation with simple integrate-and-dump operations. Unlike TR and differential schemes, however, our noncoherent algorithm allows these segments to be taken across symbols, which makes it possible to cope with mistiming. In other words, the TR and differential templates are noisy but "on-time," while our templates are both noisy and offset in time, and are thus "dirty."

To alleviate the need for a symbol synchronizer, joint sequence and timing estimation algorithms have also been investigated in the context of conventional communications [6], [7]. However, only additive noise channels were considered in developing such algorithms, which can hence assume usage of "clean" templates at the receiver. Different from [6], [7], we consider *unknown* dense multipath UWB channels which necessitates demodulating with "dirty" templates. As a result, our noncoherent algorithm bypasses not only symbol synchronization, but also multipath channel estimation.

Our noncoherent demodulator will be shown to be optimal in the maximum likelihood (ML) sense. Since it works regardless of timing offset, it can also be applied after (possibly imperfect) timing acquisition. We will show that the noncoherent demodulator reduces to a differential one when timing is perfect. The noncoherent demodulation can also be combined with a TR transmission to improve its performance in the presence of mistiming.

Paper approved by A. F. Naguib, the Editor for Wireless Communication of the IEEE Communications Society. Manuscript received December 13, 2004; revised March 22, 2006. This work was supported in part by the U.S. Army Research Laboratory through the Communications and Networks Consortium under the Collaborative Technology Alliance Program, Cooperative Agreement DAAD19-01-2-0011, in part by the NSF ITR under Grant EIA-0324864, and in part by the NSF MRI under Grant CNS-0420836. This paper was presented in part at the MILCOM Conference, Monterey, CA, October/November 2004. The U.S. Government is authorized to reproduce and distribute reprints for Government purposes notwithstanding any copyright notation thereon.

L. Yang is with the Department of Electrical and Computer Engineering, University of Florida, Gainesville, FL 32611 USA (e-mail: lqyang@ece.ufl.edu).

G. B. Giannakis is with the Department of Electrical and Computer Engineering, University of Minnesota, 200 Minneapolis, MN 55455 USA (e-mail: georgios@ece.umn.edu).

A. Swami is with the Army Research Laboratory, Adelphi, MD 20783-1197 USA (e-mail: a.swami@ieee.org).

Digital Object Identifier 10.1109/TCOMM.2007.894116

The ensuing Section II outlines our system model. Section III derives a novel noncoherent demodulation algorithm with ML optimality. An alternative conditionally ML optimal demodulator with low complexity is then established in Section IV. In Section V, a robust-to-timing TR (RTTR) UWB demodulator is developed to improve the performance of the original TR in the presence of mistiming. Simulations are presented in Section VI.

Notation: $\lfloor\cdot\rfloor$ and $\lceil\cdot\rceil$ stand for integer floor and ceiling operations; $E\{\cdot\}$ and $STD\{\cdot\}$ represent expected value and standard deviation of a random variable; $x(\mathrm{mod}y) := x - y\lfloor x/y\rfloor$ denotes both integer and real-valued modulo operations on x with base y.

II. Modeling and Problem Statement

In the impulse UWB radio, every information symbol is conveyed by N_f data modulated pulses $p(t)$ with duration T_p, one per frame of duration $T_f > T_p$. The symbol duration is thus $T_s = N_f T_f$ seconds. To smooth transmit-spectra, provide LPD and accommodate multiple users, pseudo-random time-hopping or direct-sequence (TH/DS) codes are often employed [16], [17]. DS codes modify the pulse amplitudes; while TH codes shift the pulse positions from frame to frame at multiples of the chip duration, which is defined as $T_c := T_f/N_c$ with N_c denoting the number of chips per frame. Letting a_k and $c_k \in [0, N_c - 1]$ denote the DS and TH code during the kth frame, the transmitted symbol-long waveform $p_T(t)$ containing N_f pulses is given by $p_T(t) := \sum_{k=0}^{N_f-1} a_k p(t - kT_f - c_k T_c)$, where $T_c > T_p$.

We model the multipath channel as a tapped-delay line with $(L+1)$ taps $\{\alpha_l\}_{l=0}^{L}$ and delays $\{\tau_l\}_{l=0}^{L}$. We also assume that the channel is quasi-static; that is, the coefficients and delays remain invariant over one transmission burst but are allowed to change across bursts. Focusing on a single user link, the waveform arriving at the receiver is given by

$$r(t) = \sqrt{\mathcal{E}} \sum_{n=0}^{N-1} \tilde{s}(n) \sum_{l=0}^{L} \alpha_l \cdot p_T(t - nT_s - \tau_l) + \eta(t)$$

where $\mathcal{E}$ is the transmit energy per pulse, $\eta(t)$ is the additive noise, and $\tilde{s}(n) := s(n) \cdot \tilde{s}(n-1)$ are differentially encoded symbols with $s(n)$ denoting the original binary pulse amplitude modulated (PAM) symbols and $\tilde{s}(-1) = 1$.

To isolate dispersive multipath effects from the propagation delay and clock offset (a.k.a. timing offset) τ_0, all path delays will be expressed as $\tau_{l,0} := \tau_l - \tau_0$. With this definition, we introduce the received symbol-level waveform

$$p_R(t) := \sum_{l=0}^{L} \alpha_l p_T(t - \tau_{l,0}) \tag{1}$$

which is the aggregate channel capturing the pulse shaper, receiver filter and multipath effects. Using (1), the received noisy signal simplifies to

$$r(t) = \sqrt{\mathcal{E}} \sum_{n=0}^{+\infty} \tilde{s}(n) \cdot p_R(t - nT_s - \tau_0) + \eta(t). \tag{2}$$

To establish our noncoherent UWB (de)modulation, we will select $T_f \geq \tau_{L,0} + T_p$ and $c_{N_f-1} = 0$ in order to confine the duration of $p_R(t)$ within $[0, T_s)$, and avoid inter-symbol interference (ISI). Notice that TH is still present in (2) and our analysis hereafter, since $c_{N_f-1} = 0$ is only assumed for the last frame. Although our demodulation algorithm requires zero ISI, the condition $T_f \geq \tau_{L,0} + T_p$ can be relaxed to allow for higher data rates, provided that guard frames are inserted between symbols to avoid ISI, much like zero-padding in narrowband systems. We underscore that our algorithm allows for inter-frame interference (IFI) that is introduced by TH codes and/or large channel delay spread, as long as ISI is absent. Furthermore, we will verify with simulations that our noncoherent UWB demodulator exhibits robustness even when low-to-moderate ISI is present. Without loss of generality, we also assume that the timing offset τ_0 is within a symbol duration; i.e., $\tau_0 \in [0, T_s)$.

III. ML Noncoherent UWB Demodulation

Starting from the noisy received waveform $r(t)$ with *unknown* timing offset τ_0 in (2), we will develop our ML optimal noncoherent demodulation algorithm in three steps: i) extraction of dirty templates; ii) integrate-and-dump operation; and iii) demodulation. The overall algorithm will be summarized towards the end of this section.

A. Step 1: Extract "Dirty" Templates

An observation interval consists of M segments, each with duration T_s starting at instants $t = mT_s, m = 0, 1, \ldots, M-1$. Denoted as $r_m(t)$, these symbol-long waveforms are

$$r_m(t) = r(t + mT_s), \qquad t \in [0, T_s), \;\; m \in [0, M-1]. \tag{3}$$

Substituting (2) into(3), we have $\forall\, m$

$$r_m(t) = \sqrt{\mathcal{E}} \sum_{n=0}^{+\infty} \tilde{s}(n) \cdot p_R(t - (n-m)T_s - \tau_0) + \eta_m(t) \tag{4}$$

where $\eta_m(t) := \eta(t + mT_s), \forall\, t \in [0, T_s)$. In the absence of channel induced ISI or partial response signaling, timing offset induces ISI from at most one adjacent symbol. Consequently, (4) can be simplified to

$$r_m(t) = \sqrt{\mathcal{E}} \sum_{n=0}^{1} \tilde{s}(m-n) \cdot p_R(t + nT_s - \tau_0) + \eta_m(t). \tag{5}$$

Notice that these symbol-long received segments $r_m(t)$ are not "clean," since they are not only noisy, but also delayed by the *unknown* timing offset τ_0 and distorted by the *unknown* propagation channel. It is worth clarifying that these "dirty" segments (templates) differ from the ones used in TR and differential UWB, where segments are noisy and distorted but have to be taken at the correct time instances [2], [10], [12].

B. Step 2: Integrate-and-Dump

The second step of our noncoherent demodulation algorithm consists of correlating adjacent "dirty" segments $r_m(t)$. Integrating-and-dumping the product of $r_m(t)$ and $r_{m-1}(t)$ results in symbol-rate samples

$$x(m) := \int_0^{T_s} r_m(t) r_{m-1}(t) dt. \tag{6}$$

Using (5) and the differential decoding equation $s(m) = \tilde{s}(m)\tilde{s}(m-1)$, we can re-express $x(m)$ as

$$\begin{aligned} x(m) &:= \tilde{s}(m-1)\tilde{s}(m-2)\mathcal{E}_A(\tau_0) + \tilde{s}(m)\tilde{s}(m-1)\mathcal{E}_B(\tau_0) \\ &\quad + \xi(m) \\ &= s(m-1)\mathcal{E}_A(\tau_0) + s(m)\mathcal{E}_B(\tau_0) + \xi(m) \end{aligned} \tag{7}$$

where

$$\mathcal{E}_A(\tau_0) := \mathcal{E}\int_0^{T_s} p_R^2(t+T_s-\tau_0)dt = \mathcal{E}\int_{T_s-\tau_0}^{T_s} p_R^2(t)dt$$

$$\mathcal{E}_B(\tau_0) := \mathcal{E}\int_0^{T_s} p_R^2(t-\tau_0)dt = \mathcal{E}\int_0^{T_s-\tau_0} p_R^2(t)dt$$

and $\xi(m)$ is a noise term that we will describe later in this section. Notice that their sum $\mathcal{E}_A(\tau_0) + \mathcal{E}_B(\tau_0) = \mathcal{E}_R := \mathcal{E}\int_0^{T_s} p_R^2(t)dt$ captures the energy of the aggregate channel in (1) and does not depend on the timing offset τ_0.

If one opts to estimate τ_0 using any timing offset estimator (such as the one in [1], [19], [22]) and manages to compensate for it (almost) perfectly, then $\tau_0 \approx 0$. In this case, $\mathcal{E}_A(0) \approx 0$, $\mathcal{E}_B(0) \approx \mathcal{E}_R$ and (7) boils down to $x(m) = s(m)\mathcal{E}_R + \xi(m)$, which can be readily demodulated with a slicer. In fact, (7) with $\tau_0 = 0$ shows that the differential UWB detectors in [2] and [10] can be viewed as special cases of our noncoherent approach. This differential UWB receiver is semi-coherent since it requires timing but bypasses channel estimation. However, even when synchronization is attempted, timing errors are inevitable and thus $\tau_0 \neq 0$. In this case, $\mathcal{E}_A(\tau_0)$ and $\mathcal{E}_B(\tau_0)$ are both nonzero and direct application of differential demodulation will lead to considerable performance degradation. This motivates our noncoherent UWB demodulation algorithms which account for the *unknown* timing offset, or the residual timing error τ_0.

Before deriving such algorithms, let us first investigate the noise term $\xi(m)$ in (7), which is the superposition of the following three terms:

$$\begin{aligned} \xi_1(m) &:= \sqrt{\mathcal{E}}\sum_{n=0}^{1}\tilde{s}(m-n)\int_0^{T_s} p_R(t+nT_s-\tau_0) \\ &\quad \times \eta_{m-1}(t)dt \\ \xi_2(m) &:= \sqrt{\mathcal{E}}\sum_{n=0}^{1}\tilde{s}(m-n-1)\int_0^{T_s} p_R(t+nT_s-\tau_0) \\ &\quad \times \eta_m(t)dt \\ \xi_3(m) &:= \int_0^{T_s}\eta_m(t)\cdot\eta_{m-1}(t)dt. \end{aligned}$$

With $\tilde{s}(m) \in \{\pm 1\}$ being i.i.d. and $\eta(t)$ in (2) being bandpass filtered AWGN with zero mean and double-sided power spectral density $\sigma^2/2$, straightforward extension of the derivations in [3], [23] reveals that, when $B \gg 1/T_s$, quantities $\xi_1(m)$, $\xi_2(m)$ and $\xi_3(m)$ can be approximated as uncorrelated Gaussian variables with zero mean and variances $\mathcal{E}_R\sigma^2/2$, $\mathcal{E}_R\sigma^2/2$ and $\sigma^4 BT_s/4$, respectively, where B is the double-sided bandwidth of the receiver front-end. As a result, the overall noise $\xi(m)$ in the symbol-rate sample $x(m)$ is also well modeled as zero-mean Gaussian with variance $\sigma_\xi^2 := \mathcal{E}_R\sigma^2 + \sigma^4 BT_s/4$. A couple of remarks are now in order.

Remark 1: The similarity of $\xi(m)$ in our noncoherent UWB with TR, PWAM and differential systems is not surprising, because all these systems share the same cross-correlation (integrate-and-dump) operation between noisy received segments as we use here [3], [10], [11], [23], [24]. However, our demodulation method is different in the sense that correlation of noisy segments in TR, PWAM and differential schemes requires timing synchronization; whereas no timing synchronization will be necessary for the noncoherent approaches that we will derive in the ensuing sections. In addition, correlation in TR and PWAM is performed between pilot and information-conveying waveforms, with the former generating an estimate of the aggregate channel; whereas in our method, correlation is carried out among information-conveying waveforms with the underlying channel being unknown. The absence of pilots in our setup clearly shows that, different from TR, we sacrifice no rate in our transmission.

Remark 2: We will show in Section V and verify with simulations in Section VI that TR indeed suffers from mistiming. In Section V, we will also develop what we term RTTR-UWB system by adapting our noncoherent demodulation algorithm to a TR transmission to improve performance of the original TR demodulator. It is also worth stressing that even though our scheme applies without timing synchronization, nothing prevents its application after (data-aided or non-data-aided) synchronization as a demodulation method robust against timing errors.

C. Step 3: ML Demodulation

We are now ready to perform symbol demodulation based on $x(m)$. Since generally $\tau_0 \neq 0$, each correlator output $x(m)$ entails two consecutive symbols, namely $s(m)$ and $s(m-1)$ [cf. (7)]. Indeed, $\{x(m)\}$ can be viewed as the symbol-rate sampled output of an unknown first-order ISI channel whose impulse response taps are the partial channel energies $\mathcal{E}_A(\tau_0)$ and $\mathcal{E}_B(\tau_0)$. This interesting viewpoint suggests noncoherent algorithms for joint symbol detection and estimation of the unknown equivalent channel based on the "dirty correlator" output samples in (7). It is worth emphasizing that only two equivalent channel taps are to be estimated with our noncoherent UWB setup, as opposed to hundreds of taps present in the underlying UWB physical channel.

Based on the noise-free part of $x(m)$ in (7), ML estimates of $s(m-1)$ and $s(m)$ can be formed as follows:

$$\begin{aligned} &\{\hat{s}(m-1), \hat{s}(m)\} \\ &\qquad = \arg\min_{\{s_1,s_2\}} \left| s_1\mathcal{E}_A(\tau_0) + s_2\mathcal{E}_B(\tau_0) - x(m) \right|. \end{aligned} \tag{8}$$

Viterbi's Algorithm (VA) can certainly be employed to implement (8). However, the VA requires knowledge of $\mathcal{E}_A(\tau_0)$ and $\mathcal{E}_B(\tau_0)$, which are unknown since neither timing nor channel information is available. Therefore, their estimates are needed prior to applying the demodulator in (8). To estimate $\mathcal{E}_A(\tau_0)$ and $\mathcal{E}_B(\tau_0)$, notice that with binary inputs, the equivalent two-tap channel can only generate four distinct outputs. Accordingly, with $\bar{x}(m)$ denoting the noise-free part of $x(m)$, $|\bar{x}(m)|$ can only take two values: $\mathcal{E}_R$ and $|\mathcal{E}_A(\tau_0) - \mathcal{E}_B(\tau_0)|$. In fact, we

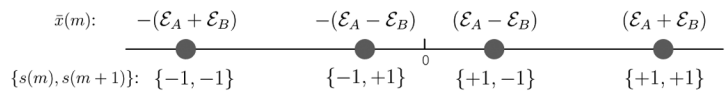

Fig. 1. $\bar{x}(m)$ and $\{s(m), s(m+1)\}$.

prove in Appendix I that $\{|\bar{x}(m)|\}$ can be treated as i.i.d. random variables with mean and standard deviation

$$\begin{aligned} E\{|\bar{x}(m)|\} &= \mathcal{E}_{\max}(\tau_0) := \max\{\mathcal{E}_A(\tau_0), \mathcal{E}_B(\tau_0)\} \\ STD\{|\bar{x}(m)|\} &= \mathcal{E}_{\min}(\tau_0) := \min\{\mathcal{E}_A(\tau_0), \mathcal{E}_B(\tau_0)\}. \end{aligned} \quad (9)$$

Naturally, these suggest the following sample estimators for $\mathcal{E}_{\max}(\tau_0)$ and $\mathcal{E}_{\min}(\tau_0)$:

$$\begin{aligned} \hat{\mathcal{E}}_{\max}(\tau_0) &:= \frac{1}{M}\sum_{m=0}^{M-1} |x(m)| \\ \hat{\mathcal{E}}_{\min}(\tau_0) &:= \sqrt{\frac{1}{M}\sum_{m=0}^{M-1}\left(|x(m)| - \hat{\mathcal{E}}_{\max}(\tau_0)\right)^2}. \end{aligned} \quad (10)$$

In order to obtain $\hat{\mathcal{E}}_A(\tau_0)$ and $\hat{\mathcal{E}}_B(\tau_0)$ from $\hat{\mathcal{E}}_{\max}(\tau_0)$ and $\hat{\mathcal{E}}_{\min}(\tau_0)$, we need an initial value to determine their relative magnitudes. To this end, we choose the first two symbols to be 1 and -1. From (7), this choice yields the noise-free sample: $\bar{x}(0) = \mathcal{E}_A(\tau_0) - \mathcal{E}_B(\tau_0)$. The sign of $\bar{x}(0)$ reveals which of $\mathcal{E}_A(\tau_0)$ and $\mathcal{E}_B(\tau_0)$ is larger, and allows one to assign to them the estimates $\hat{\mathcal{E}}_{\max}(\tau_0)$ and $\hat{\mathcal{E}}_{\min}(\tau_0)$, as we summarize next.

1) Result 1: From the estimates $\hat{\mathcal{E}}_{\max}(\tau_0)$ and $\hat{\mathcal{E}}_{\min}(\tau_0)$ in (10), and the first sample $x(0)$, energies $\mathcal{E}_A(\tau_0)$ and $\mathcal{E}_B(\tau_0)$ can be obtained in closed-form as

$$\begin{aligned} \hat{\mathcal{E}}_A(\tau_0) =& \hat{\mathcal{E}}_{\max}(\tau_0)\delta(\text{sign}\{x(0)\} - 1) \\ &+ \hat{\mathcal{E}}_{\min}(\tau_0)\delta(\text{sign}\{x(0)\} + 1) \\ \hat{\mathcal{E}}_B(\tau_0) =& \hat{\mathcal{E}}_{\max}(\tau_0)\delta(\text{sign}\{x(0)\} + 1) \\ &+ \hat{\mathcal{E}}_{\min}(\tau_0)\delta(\text{sign}\{x(0)\} - 1) \end{aligned} \quad (11)$$

where $\delta(\cdot)$ represents Kronecker's delta function.

Notice that noise may render the sign of $x(0)$ different from that of $\bar{x}(0)$. The probability for this to happen can be shown to be $Q(|\mathcal{E}_A(\tau_0) - \mathcal{E}_B(\tau_0)|/\sigma_\xi)$, where $Q(\cdot)$ is the Gaussian tail function. This probability is large when $|\mathcal{E}_A(\tau_0) - \mathcal{E}_B(\tau_0)|$ is relatively small, in which case the effects of mistakenly alternating the two is also small. As an extreme example of the latter, it does not make any difference to alternate the two when $\mathcal{E}_A(\tau_0) = \mathcal{E}_B(\tau_0)$. In cases where $|\mathcal{E}_A(\tau_0) - \mathcal{E}_B(\tau_0)|$ is much greater compared with the noise variance, an alternation between $\mathcal{E}_A(\tau_0)$ and $\mathcal{E}_b(\tau_0)$ can have considerable effect on the demodulation performance. But fortunately, the probability of an alternation is small in this case.

D. ML Noncoherent UWB Demodulation Algorithm

Over a burst of duration MT_s, our ML noncoherent demodulator follows these steps.

S1.Take symbol-long segments of the received waveform as in (3), $\forall\, m \in [0, M-1]$.

S2.Integrate-and-dump the product of every pair of neighboring segments to obtain $x(m)$, $\forall\, m \in [0, M-1]$, as in (6).

S3.Form estimates $\hat{\mathcal{E}}_A(\tau_0)$ and $\hat{\mathcal{E}}_B(\tau_0)$ using (10) and (11).

S4.Demodulate using ML sequence detectors such as Viterbi's Algorithm or its per-survivor variants (see, e.g., [15]) to tradeoff error performance for complexity.

IV. Conditional ML Noncoherent UWB Demodulation

Our ML noncoherent demodulator in the previous section is an ML sequence estimator. To further reduce its complexity, notice that each symbol $s(m)$ appears in two consecutive symbol-rate samples $x(m)$ and $x(m+1)$ [cf. (7)]. Hence, each symbol $s(m)$ has two "chances" to be demodulated, once using $x(m)$ and another time using $x(m+1)$. Based on this observation, we will use a conditional ML approach to develop a demodulator with lower complexity.

Demodulating $s(m)$ from sample $x(m+1)$ and ignoring $s(m+1)$ which has not yet been demodulated, the decision rule in (8) can be simplified to a sign detector [see (7)]

$$\hat{s}(m) = \text{sign}\{x(m+1)\}. \quad (12)$$

On the other hand, conditioned on the previous estimate $\hat{s}(m-1)$, symbol $s(m)$ can be demodulated from $x(m)$ as follows [cf. (7)]:

$$\hat{s}(m) = \arg\min_{s\in\{\pm 1\}} \left|\hat{s}(m-1)\hat{\mathcal{E}}_A(\tau_0) + s\hat{\mathcal{E}}_B(\tau_0) - x(m)\right|. \quad (13)$$

Obtained by modifying (8), the demodulator in (13) is ML optimal *conditioned* on $s(m-1)$ being correctly demodulated. It can be easily verified that (13) can be further simplified to a decision-directed form

$$\hat{s}(m) = \text{sign}\left\{x(m) - \hat{s}(m-1)\hat{\mathcal{E}}_A(\tau_0)\right\}. \quad (14)$$

In fact, the demodulator in (12) can be regarded as a *linear* equalizer; whereas the one in (14) can be regarded as a single-feedback-tap *nonlinear* decision-feedback equalizer. To optimize the demodulation performance at reduced complexity, we will select, between (12) and (14), the one incurring smaller average probability of error. To this end, let us first visualize the constellation of $\bar{x}(m)$ generated by symbol pairs $\{s(m-1), s(m)\}$ in Fig. 1. From this figure, it follows that the probabilities of erroneously demodulating $s(m)$ using the sign detector (SD) and the decision-directed (DD) rules are

$$\begin{aligned} P_{SD}(e) =& \frac{1}{2}Q\left(\frac{\mathcal{E}_R}{\sigma_\xi}\right) \\ &+ \frac{1}{2}Q\left(\frac{\mathcal{E}_A(\tau_0) - \mathcal{E}_B(\tau_0)}{\sigma_\xi}\right) \\ P_{\text{DD}}\left(e|\hat{s}(m-1)\text{ correct}\right) =& Q\left(\frac{\mathcal{E}_B(\tau_0)}{\sigma_\xi}\right). \end{aligned} \quad (15)$$

Equation (15) shows that estimation of $s(m)$ using SD or DD leads to different error rates. For instance, it is not favorable to demodulate $s(m)$ from $x(m)$ if $\mathcal{E}_B(\tau_0)$ is small, since the distance between the left and right pairs of the constellation points in Fig. 1 is also small. On the other hand, it is not desirable to demodulate $s(m)$ from $x(m+1)$ if the difference $|\mathcal{E}_A(\tau_0) - \mathcal{E}_B(\tau_0)|$ is small, because the two center points are getting closer in Fig. 1.

To obtain reliable error performance, one should always choose between (12) and (14) the one corresponding to $\min\{P_{SD}(e), P_{\rm DD}(e|\hat{s}(m-1) \text{ correct})\}$. From (15), it is clear that such a choice depends on $\mathcal{E}_A(\tau_0)$, $\mathcal{E}_B(\tau_0)$ and the effective signal-to-noise ratio (SNR) $\mathcal{E}_R/\sigma_\xi$. Since estimates of $\mathcal{E}_A(\tau_0)$ and $\mathcal{E}_B(\tau_0)$ can be formed as in (11), it is natural—and will be shown possible—to choose between (12) and (14) according to the ratio $\rho_{ba} := \mathcal{E}_B(\tau_0)/\mathcal{E}_A(\tau_0)$. When $\rho_{ba} < 1$, the two-tap channel is maximum-phase and vice versa. At first glance, it appears that one should prefer SD if the channel is maximum-phase and DD if it is minimum-phase, as the DD demodulator has been shown to perform poorly when the channel is non-minimum phase (see, e.g., [13]). However, the optimal ρ_{ba} turns out to depend on the ratio $\mathcal{E}_R/\sigma_\xi$. For this reason, we will resort to a suboptimum but simple relationship between ρ_{ba} and the choice between (12) and (14). Specifically, we will prove the following.

1) Result 2: For any $\mathcal{E}_R$ and σ_ξ, we have

$$P_{SD}(e) < P_{\rm DD}(e|\hat{s}(m-1) \text{ correct}) \qquad \forall\, \rho_{ba} \in [0, 0.5]$$
$$P_{SD}(e) > P_{\rm DD}(e|\hat{s}(m-1) \text{ correct}) \qquad \forall\, \rho_{ba} \in [1, +\infty).$$

Proof: See Appendix II.

As a direct implication of Result 2, if a channel and a timing offset τ_0 lead to $\rho_{ba} \leq 0.5$, then all symbols should be estimated using (12); if $\rho_{ba} > 1$, then (14) should be used. Although the situation is not as clear-cut for $\rho_{ba} \in (0.5, 1)$, high SNR is beneficial for (14) because one can make use of the previous estimate, as will be detailed later; whereas at low SNR, estimates $\hat{\mathcal{E}}_A(\tau_0)$ and $\hat{\mathcal{E}}_B(\tau_0)$ are not reliable anyway. Based on these considerations, we choose 0.5 as the threshold for ρ_{ba}; that is, symbols should be estimated using (12) if $\rho_{ba} \leq 0.5$, and using (14) otherwise. Notice that both conditional ML (CML) demodulators in (12) and (14) can be implemented with a single slicer and incur lower complexity than the ML sequence detector in (8).

It is worth stressing that, instead of pursuing an $\mathcal{E}_R/\sigma_\xi$-dependent threshold, one can decide whether to use (12) or (14) by simply comparing ρ_{ba} with 0.5. In our simulations, we will see that setting the cutoff point at $\rho_{ba} = 0.5$ achieves close-to-optimum BER performance; whereas setting $\rho_{ba} = 1$ (i.e., separating the minimum versus maximum-phase channels) results in considerable performance degradation.

As expected, with perfect timing ($\tau_0 = 0$), we have $\mathcal{E}_A(\tau_0) = 0$. The (conditional) ML decision rules (8), (12) and (14) simplify to a differential UWB demodulator

$$\hat{s}(m) = \text{sign}\{x(m)\}. \tag{16}$$

A. CML Noncoherent UWB Demodulation Algorithm

Over a burst of duration MT_s, our CML noncoherent demodulator follows these steps.

S1.Take symbol-long segments of the received waveform as in **(3)**, $\forall\, m \in [0, M-1]$.

S2.Integrate-and-dump the product of every pair of neighboring segments to obtain $x(m)$, $\forall\, m \in [0, M-1]$, as in **(6)**.

S3.Form estimates $\hat{\mathcal{E}}_A(\tau_0)$ and $\hat{\mathcal{E}}_B(\tau_0)$ using **(10)** and **(11)**.

S4.If $\hat{\rho}_{ba} = \hat{\mathcal{E}}_B(\tau_0)/\hat{\mathcal{E}}_A(\tau_0) \leq 0.5$, demodulate $s(m)$, $\forall\, m \in [2, M-1]$ as in **(12)** and $s(M)$ as in **(14)**; otherwise, demodulate $s(m)$, $\forall\, m \in [2, M]$ based on **(14)**.

Remark 3: Although our noncoherent symbol demodulation algorithms are developed without performing timing synchronization, they can certainly be applied after one acquires timing with pilots or blindly. In such cases, τ_0 corresponds to residual timing errors. In addition, our algorithm can be adapted to a TR setting, which will be shown next to considerably improve the bit-error-rate (BER) performance of TR in the presence of unknown timing offset or timing error.

Remark 4: The proposed implementation requires a single analog delay element, with a delay of T_s; further, digital sampling needs to be done only at the symbol rate T_s, not the frame rate T_f or chip rate T_c.

V. Robust-to-Timing Transmitted Reference (RTTR) UWB

In the conventional TR UWB system,[1] each information-conveying waveform is accompanied by a pilot waveform, as depicted in Fig. 2. Upon reception, the received pilot waveforms are delayed by one frame duration T_f and correlated with their adjacent information-conveying waveforms. A total of $N_f/2$ correlation outputs corresponding to a single symbol are then accumulated to form symbol-rate samples which in turn serve as decision statistics. When perfect timing is achieved as shown in Fig. 2(a), the delayed pilot waveforms are perfectly aligned with the information-conveying ones. The symbol-rate sample corresponding to the mth symbol is then given by

$$x(m) = \frac{\mathcal{E}_R}{2} s(m) + \xi(m) \tag{17}$$

where we used the fact that the energy of each received frame-level waveform is $\mathcal{E}_R/N_f$ in the absence of TH. Notice that since integration is performed over $N_f/2$ frames, the variance of the noise term $\xi(m)$ is now $\sigma_\xi^2/2$. Based on the symbol-rate samples in (17), the original TR demodulator is simply a sign detector

$$\hat{s}(m) = \text{sign}\{x(m)\}. \tag{18}$$

[1]Recently, energy and bandwidth efficient versions of TR have been proposed (see, e.g., [23]). However, these improved versions do not share the relaxed timing requirement that the original TR has. For this reason, we will consider here only the conventional TR.

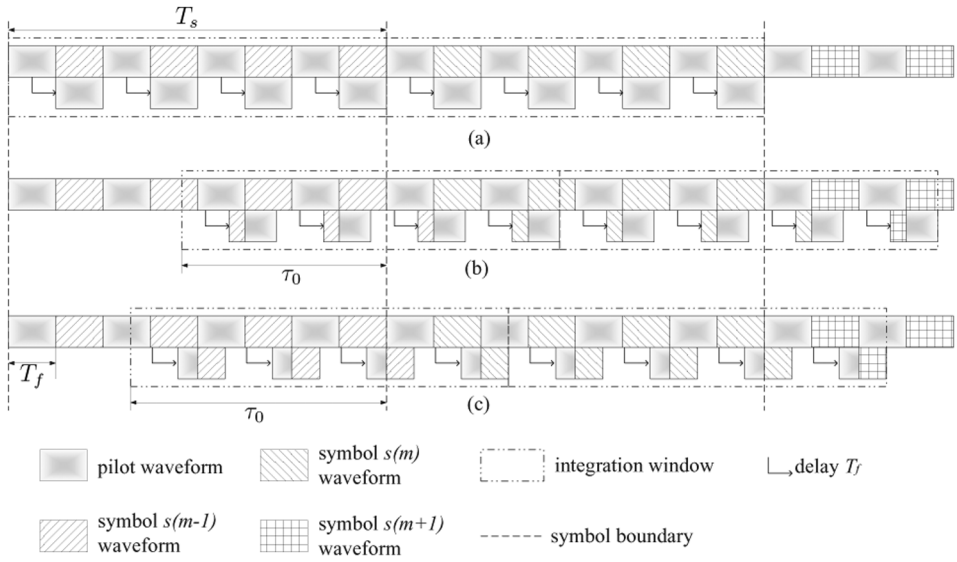

Fig. 2. First step S1 of a (RT)TR receiver with (a) perfect timing; (b) unknown τ_0 such that $\lfloor \tau_0/T_f \rfloor$ is even; and (c) unknown τ_0 such that $\lfloor \tau_0/T_f \rfloor$ is odd. $(N_f = 8)$.

Nevertheless, the symbol-rate samples $x(m)$ will have a form different from (17) when timing offset or residual errors $\tau_0 \neq 0$ are present. In Sections V-A and B, we will investigate the sensitivity of such a UWB modem with respect to unknown timing offset or timing error.

A. Timing Sensitivity of TR-UWB

If $\lfloor \tau_0/T_f \rfloor$ is an even number, then the integration window boundaries fall into information-conveying waveforms, as shown in Fig. 2(b), and $x(m)$ becomes

$$x(m) = \left[\frac{N_\tau}{N_f}\mathcal{E}_R - \mathcal{E}_B(T_s - \tau_f)\right] s(m-1) + \left[\left(\frac{1}{2} - \frac{N_\tau}{N_f}\right)\mathcal{E}_R + \mathcal{E}_B(T_s - \tau_f)\right] s(m) + \xi(m) \quad (19)$$

where $\mathcal{E}_B(T_s - \tau_f) = \mathcal{E}\int_0^{\tau_f} p_R^2(t)dt$ by definition, $N_\tau := \lceil \tau_0/(2T_f) \rceil$ and $\tau_f := T_f - \tau_0 (\mathrm{mod}\ T_f)$ can be interpreted as the symbol-level and frame-level timing offset, respectively.

If $\lfloor \tau_0/T_f \rfloor$ is an odd number, then the integration window boundaries fall into pilot waveforms, as shown in Fig. 2(c), and symbol-rate samples obey

$$x(m) = \frac{N_\tau}{N_f}\mathcal{E}_R \cdot s(m-1) + \left(\frac{1}{2} - \frac{N_\tau}{N_f}\right)\mathcal{E}_R \cdot s(m) + \xi(m). \quad (20)$$

Combining (19) and (20), we obtain a general form of symbol-rate samples in a TR-UWB system with timing offset τ_0

$$x(m) = \tilde{\mathcal{E}}_A(\tau_0) \cdot s(m-1) + \tilde{\mathcal{E}}_B(\tau_0) \cdot s(m) + \xi(m), \quad (21)$$

where

$$\tilde{\mathcal{E}}_A(\tau_0) := \begin{cases} \frac{N_\tau}{N_f}\mathcal{E}_R - \mathcal{E}_B(T_s - \tau_f), & \text{if } \left\lfloor \frac{\tau_0}{T_f} \right\rfloor \text{ is even} \\ \frac{N_\tau}{N_f}\mathcal{E}_R, & \text{if } \left\lfloor \frac{\tau_0}{T_f} \right\rfloor \text{ is odd} \end{cases}$$

and

$$\tilde{\mathcal{E}}_B(\tau_0) := \begin{cases} \left(\frac{1}{2} - \frac{N_\tau}{N_f}\right)\mathcal{E}_R + \mathcal{E}_B(T_s - \tau_f), & \left\lfloor \frac{\tau_0}{T_f} \right\rfloor \text{ even} \\ \left(\frac{1}{2} - \frac{N_\tau}{N_f}\right)\mathcal{E}_R, & \left\lfloor \frac{\tau_0}{T_f} \right\rfloor \text{ odd.} \end{cases}$$

Notice that when $\lfloor \tau_0/T_f \rfloor$ is odd, symbol-rate samples are *insensitive* to the frame-level offset τ_f. In particular, when $\tau_0 \in [T_s - T_f, T_s)$, we have $N_\tau = N_f/2$ and $\tau_f \in [0, T_f)$. Equation (20) yields $x(m) = (\mathcal{E}_R/2) \cdot s(m-1) + \xi(m)$, which is essentially the same as (17). This shows that TR-UWB relaxes timing requirements to some extent, essentially because a reference pulse is placed both before and after a data pulse. However, in the presence of timing offset/error, (21) shows that the original TR demodulator in (18) will inevitably give rise to considerable performance degradation—a fact that we will corroborate with simulations.

These considerations motivate our subsequent development of a robust-to-timing (RT) TR scheme. In the presence of *unknown* timing offset (or timing error) τ_0, (21) that models the input–output (I/O) relationship of TR-UWB bears the same form as (7).

B. RTTR-UWB

The transmitter of our RTTR-UWB is identical to that in a conventional TR-UWB system; that is, each symbol is transmitted over N_f waveforms, out of which $N_f/2$ pilot waveforms and $N_f/2$ information-conveying ones are interleaved. Upon reception, after *optional* timing synchronization, our RTTR demodulator follows these steps.

S1.Over each symbol duration $[mT_s, (m+1)T_s)$, take frame (T_f)-long segments of the received waveform, correlate $N_f/2$ pairs of these segments, and accumulate the correlator outputs to obtain $x(m)$ as in (21), $\forall\, m \in [0, M-1]$.

S2.Form estimates $\hat{\tilde{\mathcal{E}}}_A(\tau_0)$ and $\hat{\tilde{\mathcal{E}}}_B(\tau_0)$ using (10) and (11).

S3.Trading off optimality for complexity reduction, implement either S3a or S3b.

S3a.Demodulate using ML sequence detection (VA or per-survivor processing).

S3b.If $\hat{\rho}_{ba} \leq 0.5$, demodulate $s(m), \forall\, m \in [2, M-1]$ as in (12) and $s(M)$ via **(14)**; otherwise, demodulate $s(m)$, $\forall\, m \in [2, M]$ as in **(14)**.

Notice that the first step of our RTTR demodulation coincides with the original TR-UWB. Although the original TR-UWB uses the sign detector in (18) in lieu of steps S2 and S3, the low-complexity option S3b for our RTTR-UWB is also essentially a sign detector.

VI. Simulations

In this section, we will compare our noncoherent demodulation algorithms with TR and differential (DIFF) UWB, which bypass channel estimation but require timing information (hence their characterization as semi-coherent). Coherent symbol demodulation is also possible with a Rake receiver which has often been tested under the assumptions of perfect timing, perfect channel delay and perfect tap estimation [20]. However, when timing and/or channel estimates are imperfect, performance of coherent demodulators can be affected considerably. Comparisons between TR and Rake receivers with imperfect channel estimates have been performed in [4]. Even under the assumptions of perfect synchronization and perfect estimation of channel tap delays, TR can outperform Rake in certain cases. When timing and channel tap delay estimation errors are not negligible, performance of the Rake receiver is expected to further degrade [18]. Given these existing comparisons between coherent Rake versus semi-coherent UWB receivers (TR and DIFF), it suffices to compare our algorithms only with TR and DIFF.

In our simulations, a Gaussian monocycle with duration $T_p = 1.0$ ns is used as the pulse shaper $p(t)$. The number of frames per symbol is $N_f = 32$. Two frame durations are selected: $T_f = 35$ ns avoids ISI; and $T_f = 5$ ns leads to considerable ISI involving two consecutive symbols. The multipath channels are generated using the channel model in [5] with real channel taps and parameters $(1/\Lambda, 1/\lambda, \Gamma, \gamma) = (43, 0.4, 7.1, 4.3)$ ns, where Λ and λ are the Poisson arrival rates of the clusters and rays within clusters, and Γ and γ are the exponential decaying factor of the mean power of the multipath arrivals. The TH codes are generated independently from a uniform distribution over $[0, N_c - 1]$ with $N_c = 35$ and $T_c = 1$ ns. Timing offsets τ_0 are uniformly distributed over $[0, T_s)$. When timing synchronization is also performed, the "dirty" template based acquisition algorithm of [21] is used with 4 training symbols, 2 out of which can also be used for estimating $\mathcal{E}_A(\tau_0)$ and $\mathcal{E}_B(\tau_0)$.

In Fig. 3, we plot the BER of our noncoherent demodulation algorithm in the absence of TH. If it is known at the receiver that perfect timing has been achieved, our CML demodulator simplifies to(16), as in the differential (DIFF) UWB of [2], [10]. The simulated BER for the DIFF scheme is about 1dB better than that of TR because the latter suffers from energy loss. Moreover, DIFF-UWB also outperforms both VA and CML based noncoherent demodulators. When timing is perfect, decision should

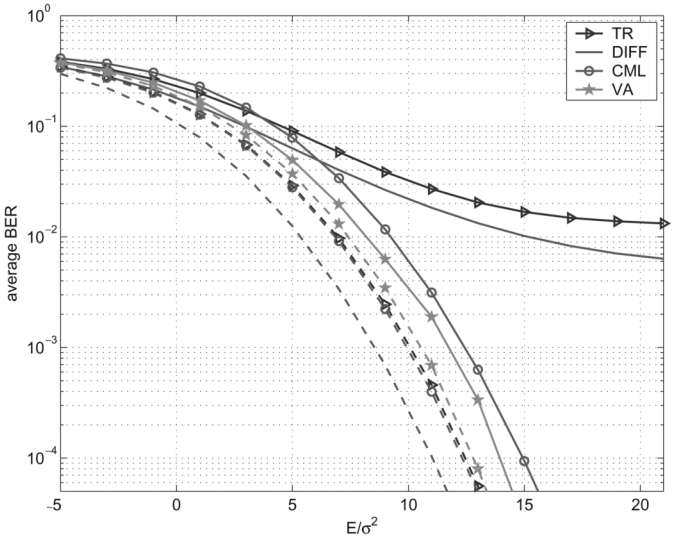

Fig. 3. BER in the presence (solid curves) and absence (dashed curves) of timing offset.

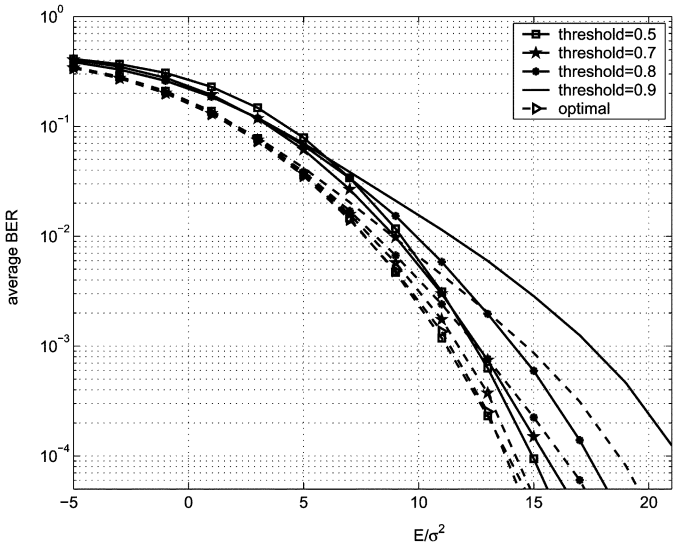

Fig. 4. Simulated BER (solid) and lower bounds (dashed) of noncoherent demodulation with various threshold values, in the presence of timing offset.

be made using $\mathcal{E}_B(0)$ alone since $\mathcal{E}_A(0) = 0$. DIFF-UWB detector does so by design; whereas VA and CML demodulators always assume imperfect timing and attempt to form $\hat{\mathcal{E}}_A(0)$ and $\hat{\mathcal{E}}_B(0)$, which introduce BER degradation. In addition, CML outperforms VA in this case, as it discards small $\hat{\mathcal{E}}_A(0)$. When no synchronization effort is made, both DIFF and TR exhibit considerable performance degradation. But with our low-complexity CML noncoherent demodulator, the degradation of the 'no timing' case from the 'perfect timing' one is about 2.5 dB. With the optimal ML demodulator using VA, performance can be further improved by 1 dB.

To verify our choice of 0.5 as the threshold in choosing between (12) and (14), we depict the average BER corresponding to five different threshold values (0.4, 0.5, 0.7, 0.8 and 0.9) in Fig. 4. Clearly, the choice of 0.5 outperforms all others for most SNR values. To further test its optimality, we also plot the BER

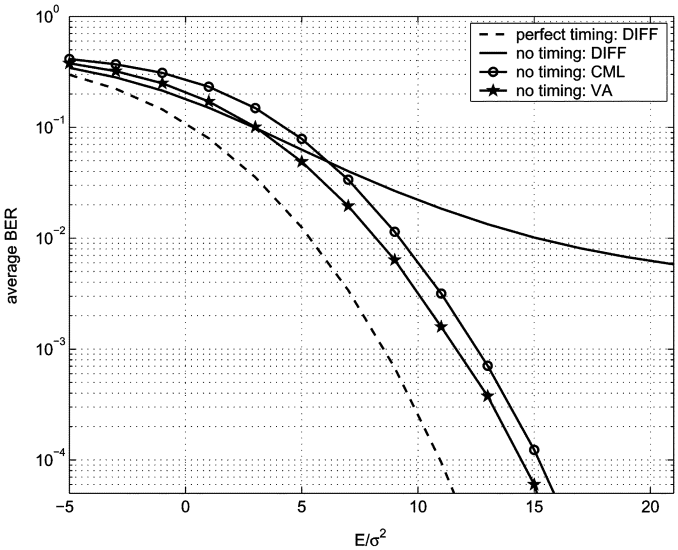

Fig. 5. BER in the presence of TH and timing offset.

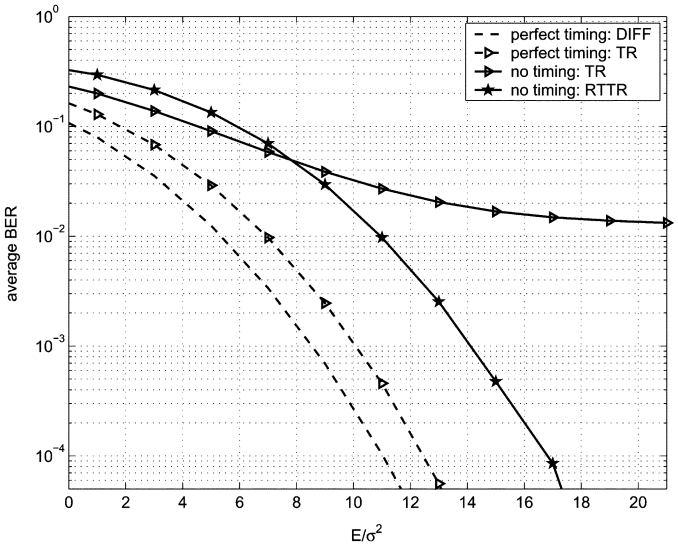

Fig. 6. BER of original TR- and RTTR-UWB, in the presence of timing offset. Conditional ML (CML) demodulation is used for RTTR.

lower bounds for all these choices. These lower bounds are calculated according to (15), assuming error-free demodulation of preceding symbols and perfect $\hat{\mathcal{E}}_A(\tau_0)$ and $\hat{\mathcal{E}}_B(\tau_0)$ estimates. The lower bound corresponding to the threshold of 0.5 again outperforms all others. All these bounds obtained with constant threshold values are further lower bounded by the one generated by choosing the minimum of the two probabilities in (15). The latter is also plotted in Fig. 4. Notice that it is almost identical to the BER lower bound corresponding to the 0.5 threshold.

When TH is also present, the BER corresponding to our noncoherent UWB is plotted in Fig. 5 for various scenarios. Comparing to Fig. 3 where TH is not used, no significant difference is observed.

In the absence and presence of timing offset, the performance of original TR and our RTTR is plotted in Fig. 6. While TR seems not operational in the presence of timing offset, our RTTR provides a simple-yet-effective remedy that exhibits considerable performance improvement at medium-to-high SNR. Fig. 6

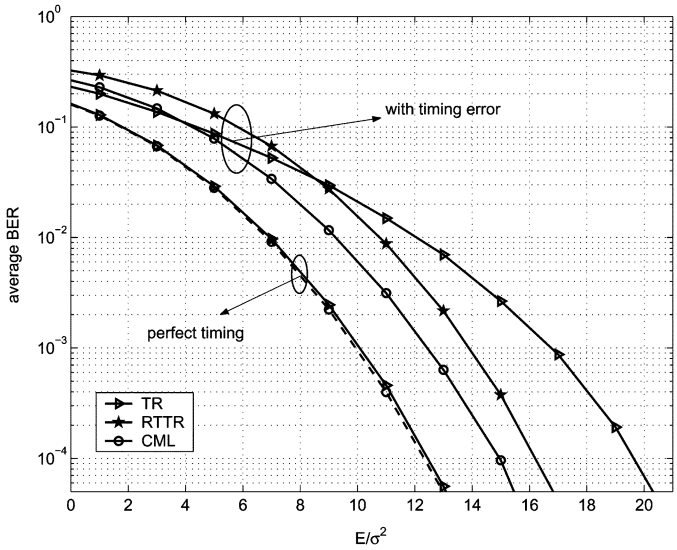

Fig. 7. BER of original TR, RTTR and noncoherent UWB, in the presence of timing synchronization error. CML demodulation is used for both noncoherent and RTTR-UWB.

shows that the original TR has a BER curve that flattens at 10^{-2}, while the BER curve for the RTTR has the same slope as those with perfect timing. Notice that the latter requires extra energy and/or bandwidth in order to achieve perfect timing.

As mentioned before, our noncoherent demodulation algorithm can be applied after timing synchronization and can amend the effects of residual timing errors. In Fig. 7, we compare the performance of original TR, our RTTR and CML noncoherent demodulation schemes in the presence of timing errors due to imperfect timing synchronization. Comparing these results with Fig. 6, the performance of the original TR is improved considerably thanks to timing synchronization. However, even this improved performance is still inferior to that of the RTTR without synchronization. Notice that the performance of RTTR is 1dB worse than that of CML noncoherent scheme, in the presence of timing error. The reason is that though RTTR improves demodulation performance, 50% energy loss is inherent to the TR transmission.

In the presence of TH and with $T_f = 5$ ns, ISI will emerge on top of IFI. In this scenario, and with timing offset, we plot the BER of our noncoherent demodulators in Fig. 8. Again, no significant performance degradation is observed.

VII. Conclusions

In this paper, we designed and tested an ML optimal *noncoherent* UWB demodulation algorithm and low complexity suboptimal alternatives to bypass timing synchronization and channel estimation. Similar to TR and differential UWB, our noncoherent demodulation relies on simple cross-correlation (integrate-and-dump) operations. But different from them, the correlation templates are not only noisy, but also offset in time. As it remains operational regardless of unknown timing offsets, our noncoherent demodulator can be applied to improve BER performance with imperfect timing acquisition. It subsumes differential UWB as a special case, and reduces to the latter when perfect timing is achieved. We

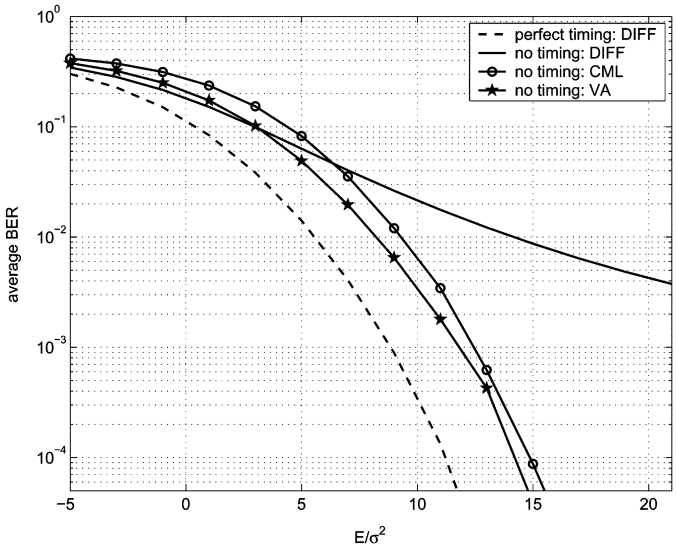

Fig. 8. BER in the presence of TH, ISI and timing offset.

also developed a RTTR-UWB system that relies on the same transmission scheme as TR-UWB, but considerably improves its performance in the presence of timing errors. As existing semi-coherent demodulators based on the auto-correlation among segments of the received noisy signal, it may be desirable to optimize the integration interval to reduce the noise effects (see, e.g., [8], [9]), especially when the frame duration exceeds the channel delay spread. This with the additional timing challenge it may induce, is a potential direction for future research.

Appendix A
Proof of (9)

First, we will show that $\{|\bar{x}(m)|\}$ can be treated as i.i.d. random variables. The unconditional probability mass function (PMF) of $|\bar{x}(m)|$ can be obtained as

$$f(|\bar{x}(m)|) = \frac{1}{2}\delta\left(|\bar{x}(m)| - \mathcal{E}_R\right) + \frac{1}{2}\delta\left(|\bar{x}(m)| - |\mathcal{E}_A(\tau_0) - \mathcal{E}_B(\tau_0)|\right). \quad (22)$$

Moreover, it follows from the structure of $\bar{x}(m)$ that its PMF conditioned on $\{|\bar{x}(k)|\}_{k<m}$ is given by $f\left(|\bar{x}(m)| \mid \{|\bar{x}(k)|\}_{k<m}\right) = f(|\bar{x}(m)| \mid s(m))$. It can also be easily verified that

$$|\bar{x}(m)| = \begin{cases} \mathcal{E}_R, & \text{if } s(m+1) = s(m), \\ |\mathcal{E}_A(\tau_0) - \mathcal{E}_B(\tau_0)|, & \text{if } s(m+1) \neq s(m), \end{cases}$$

regardless of the value of $s(m)$. With i.i.d. binary PAM symbols, the events $s(m+1) = s(m)$ and $s(m+1) \neq s(m)$ occur with equal probability $1/2$. Therefore, the conditional PMF of $|\bar{x}(m)|$ is the same as its unconditional PMF

$$f\left(|\bar{x}(m)| \mid \{|\bar{x}(k)|\}_{k<m}\right) = f(|\bar{x}(m)|)$$

which implies that $|\bar{x}(m)|$ is independent of all previous samples $\{|\bar{x}(k)|\}_{k<m}$. Since this is true $\forall\ m$, we deduce that $\{|\bar{x}(m)|\}$ are i.i.d. random variables with PMF as in (22).

Mean and variance of $|\bar{x}(m)|$ can then be obtained respectively as

$$\begin{aligned} &E\{|\bar{x}(m)|\} \\ &\quad = \frac{1}{2}\left(\mathcal{E}_R + |\mathcal{E}_A(\tau_0) - \mathcal{E}_B(\tau_0)|\right) \\ &\quad = \begin{cases} \mathcal{E}_A(\tau_0), & \text{if } \mathcal{E}_A(\tau_0) \geq \mathcal{E}_B(\tau_0) \\ \mathcal{E}_B(\tau_0), & \text{otherwise} \end{cases} \\ &\qquad\qquad \text{and} \\ &E\{|\bar{x}(m)|^2\} - E^2\{|\bar{x}(m)|\} \\ &\quad = \begin{cases} \frac{1}{2}\left(\mathcal{E}_R^2 + |\mathcal{E}_A(\tau_0) - \mathcal{E}_B(\tau_0)|^2\right) - \mathcal{E}_A^2(\tau_0) \\ \frac{1}{2}\left(\mathcal{E}_R^2 + |\mathcal{E}_A(\tau_0) - \mathcal{E}_B(\tau_0)|^2\right) - \mathcal{E}_B^2(\tau_0) \end{cases} \\ &\quad = \begin{cases} \mathcal{E}_B^2(\tau_0), & \text{if } \mathcal{E}_A(\tau_0) \geq \mathcal{E}_B(\tau_0) \\ \mathcal{E}_A^2(\tau_0), & \text{otherwise.} \end{cases} \end{aligned}$$

Equation (9) then follows upon defining $\mathcal{E}_{\max} := \max\{\mathcal{E}_A(\tau_0), \mathcal{E}_B(\tau_0)\}$ and $\mathcal{E}_{\min}(\tau_0) := \min\{\mathcal{E}_A(\tau_0), \mathcal{E}_B(\tau_0)\}$.

Appendix B
Proof of Result 2

To prove Result 2, we first re-express the probabilities of error in (15) in terms of the ratio $\rho_{ba} := \mathcal{E}_B(\tau_0)/\mathcal{E}_A(\tau_0)$ as

$$\begin{aligned} {}_{\mathrm{DD}}(e|\hat{s}(m-1) \text{ correct}) &= Q\left(\rho \cdot \frac{\rho_{ba}}{1+\rho_{ba}}\right) \\ P_{SD}(e) &= \frac{1}{2}Q(\rho) + \frac{1}{2}Q\left(\rho \cdot \frac{1-\rho_{ba}}{1+\rho_{ba}}\right) \end{aligned}$$

where $\rho := \mathcal{E}_R/\sigma_\xi$. For $\rho_{ba} \in [0, 0.5]$, we have $(1-\rho_{ba}) \geq \rho_{ba}$ and thus

$$Q(\rho) \leq Q\left(\rho \cdot \frac{1-\rho_{ba}}{1+\rho_{ba}}\right) \leq Q\left(\rho \cdot \frac{\rho_{ba}}{1+\rho_{ba}}\right) \qquad \forall\ \rho > 0. \quad (23)$$

On the one hand, the left equality of (23) holds if and only if $\rho_{ba} = 0$; that is, $\mathcal{E}_B(\tau_0) = 0$. On the other hand, the right equality of (23) holds if and only if $\rho_{ba} = 0.5$; that is, $\mathcal{E}_A(\tau_0) = 2\mathcal{E}_B(\tau_0)$. Therefore, the two equalities can not hold simultaneously. As a result, we have the strict inequality $P_{SD}(e) < P_{\mathrm{DD}}(e|\hat{s}(m-1) \text{ correct})$.

When $\rho_{ba} > 1$, utilizing the convexity of the Q function, we find

$$\begin{aligned} Q\left(\frac{\rho}{2}\left(1 + \frac{\rho_{ba}-1}{1+\rho_{ba}}\right)\right) &< \frac{1}{2}Q(\rho) + \frac{1}{2}Q\left(\rho \cdot \frac{\rho_{ba}-1}{1+\rho_{ba}}\right) \\ &< \frac{1}{2}Q(\rho) + \frac{1}{2}Q\left(\rho \cdot \frac{1-\rho_{ba}}{1+\rho_{ba}}\right) \\ &\quad \forall\ \rho \end{aligned}$$

where the left-hand side of the inequality turns out to be $P_{\mathrm{DD}}(e|\hat{s}(m-1) \text{ correct})$, and the right-hand side equals $P_{SD}(e)$.

REFERENCES

[1] R. Blazquez, P. Newaskar, and A. Chandrakasan, "Coarse acquisition for ultra-wideband digital receivers," in *Proc. Int. Conf. Acoust., Speech, Signal Process.*, Hong Kong, China, Apr. 6–10, 2003, pp. 137–140.

[2] Y. Chao and R. A. Scholtz, "Optimal and suboptimal receivers for ultra-wideband transmitted reference systems," in *Proc. Global Telecommun. Conf.*, San Francisco, CA, Dec. 1–5, 2003, pp. 744–748.

[3] J. D. Choi and W. E. Stark, "Performance of ultra-wideband communications with suboptimal receivers in multipath channels," *IEEE J. Sel. Areas Commun.*, vol. 20, no. 12, pp. 1754–1766, Dec. 2002.

[4] M.-H. Chung and R. A. Scholtz, "Comparison of transmitted- and stored-reference systems for ultra-wideband communications," in *Proc. MILCOM Conf.*, Monterey, CA, Oct. 3, 2004.

[5] J. R. Foerster, "Channel Modeling Sub-Committee Report: Final," Working Group for WPAN, IEEE P802.15–02/368r5-SG3a, IEEE P802.15, 2002.

[6] C. N. Georghiades, "Optimum delay and sequence estimation from incomplete data," *IEEE Trans. Inf. Theory*, vol. 36, no. 1, pp. 202–208, Jan. 1990.

[7] C. N. Georghiades and M. Moeneclaey, "Sequence estimation and synchronization from nonsynchronized samples," *IEEE Trans. Inf. Theory*, vol. 37, no. 6, pp. 1649–1657, Nov. 1991.

[8] N. He and C. Tepedelenlioglu, "Adaptive synchronization for non-coherent UWB receivers," in *Proc. Int. Conf. Acoust., Speech, Signal Process.*, Montreal, QC, Canada, May 17–29, 2004, pp. 517–520.

[9] N. He and C. Tepedelenlioglu, "Performance analysis of non-coherent UWB receivers at different synchronization levels," in *Proc. Global Telecommun. Conf.*, Dallas, TX, Nov.–Dec. 2004, pp. 3517–3521.

[10] M. Ho, V. Somayazulu, J. Foerster, and S. Roy, "A differential detector for an ultra-wideband communications system," in *Proc. Veh. Technol. Conf.*, Birmingham, AL, May 2002, pp. 1896–1900.

[11] R. T. Hoctor and H. W. Tomlinson, "Delay-hopped transmitted-reference RF communications," in *Proc. IEEE Conf. Ultra-Wideband Syst. Technol.*, Baltimore, MD, May 2002, pp. 265–269.

[12] R. T. Hoctor and H. W. Tomlinson, "An overview of delay-hopped, transmitted-reference RF communications," in *G.E. Res. Dev. Center, Tech. Inf. Ser.*, Jan. 2002, pp. 1–29.

[13] A. Leclert and P. Vandamme, *Decision Feedback Equal, Dispersive Radio Channels*, vol. 33, no. 7, pp. 676–684, Jul. 1985.

[14] D. Porrat and D. Tse, "Bandwidth scaling in ultra-wideband communications," in *Proc. 41st Allerton Conf.*, Monticello, IL, Oct. 2003.

[15] R. Raheli, A. Polydoros, and C. K. Tzou, "Per-survivor processing: A general approach to MLSE in uncertain environments," *IEEE Trans. Commun.*, vol. 44, no. 2-4, pp. 354–364, Feb.-Apr. 1995.

[16] B. M. Sadler and A. Swami, "On the performance of UWB and DS-spread spectrum communication systems," in *Proc. IEEE Conf. Ultra-Wideband Syst. Technol.*, Baltimore, MD, May 2002, pp. 289–292.

[17] R. A. Scholtz, "Multiple access with time-hopping impulse modulation," in *Proc. MILCOM Conf.*, Boston, MA, Oct. 1993, pp. 447–450.

[18] H. Sheng, R. You, and A. M. Haimovich, "Performance analysis of ultra-wideband Rake receivers with channel delay estimation errors," in *Proc. Conf. Inf. Sci. Syst.*, Mar. 2004, pp. 921–926.

[19] Z. Tian and G. B. Giannakis, "Data-aided ML timing acquisition in ultra-wideband radios," in *Proc. IEEE Conf. Ultra-Wideband Syst. Technol.*, Reston, VA, Nov. 2003, pp. 142–146.

[20] M. Z. Win, G. Chrisikos, and N. R. Sollenberger, "Performance of Rake reception in dense multipath channels: Implications of spreading bandwidth and selection diversity order," *IEEE J. Sel. Areas Commun.*, vol. 18, no. 8, pp. 1516–1525, Aug. 2000.

[21] L. Yang and G. B. Giannakis, "Low-complexity training for rapid timing acquisition in ultra-wideband communications," in *Proc. Global Telecommun. Conf.*, San Francisco, CA, Dec. 2003, pp. 769–773.

[22] L. Yang and G. B. Giannakis, "Timing ultra-wideband signals with dirty templates," *IEEE Trans. Commun.*, vol. 53, no. 11, pp. 1952–1963, Nov. 2005.

[23] L. Yang and G. B. Giannakis, "Optimal pilot waveform assisted modulation for ultra-wideband communications," *IEEE Trans. Wireless Commun.*, vol. 3, no. 4, pp. 1236–1249, Jul. 2004.

[24] H. Zhang and D. L. Goeckel, "Generalized transmitted-reference UWB systems," in *Proc. IEEE Conf. Ultra-Wideband Syst. Technol.*, Reston, VA, Nov. 2003, pp. 147–151.

Liuqing Yang (SM'06) received the B.S. degree in electrical engineering from Huazhong University of Science and Technology, Wuhan, China, in 1994, and the M.Sc. and Ph.D. degrees in electrical and computer engineering from the University of Minnesota, Minneapolis, in 2002 and 2004, respectively.

Since August 2004, she has been an Assistant Professor in the Department of Electrical and Computer Engineering, University of Florida, Gainesville. Her general interests include communications and signal processing, communications theory and networking. Her current research focuses on ultra-wideband wireless communication systems, diversity techniques for conventional communication systems and distributed and cooperative wireless networks, synchronization and channel estimation, multiple access, space-time coding, and single/multi-carrier systems.

Dr. Yang was the recipient of the Best Dissertation Award in the Physical Sciences and Engineering from the University of Minnesota.

Georgios B. Giannakis (F'97) received the Diploma in Electrical Engr. from the National Technical University of Athens, Athens, Greece, in 1981, the M.Sc. degree in electrical engineering, the M.Sc. degree in mathematics, and the Ph.D. degree in electrical engineering, 1986. from the University of Southern California (USC), San Diego, in 1983, 1986, and 1986, respectively.

Since 1999, he has been a Professor with the Department of Electrical and Computer Engineering, University of Minnesota, Minneapolis, where he now holds an ADC Chair in Wireless Telecommunications. His general interests span the areas of communications, networking and statistical signal processing—subjects on which he has published more than 250 journal papers, 450 conference papers, two edited books and two research monographs *Space-Time Coding for Broadband Wireless Communications* (Wiley 2006) and *Ultra-Wideband Wireless Communications* (Cambridge Press 2007). His current research focuses on diversity techniques, complex-field and space-time coding, multicarrier, cooperative wireless communications, cognitive radios, cross-layer designs, mobile ad hoc networks, and wireless sensor networks.

Dr. Giannakis is the (co-) recipient of six paper awards from the IEEE Signal Processing (SP) and Communications Societies including the G. Marconi Prize Paper Award in Wireless Communications. He also received Technical Achievement Awards from the SP Society (2000), from EURASIP (2005), a Young Faculty Teaching Award and the G. W. Taylor Award for Distinguished Research from the University of Minnesota. He has served the IEEE in a number of posts.

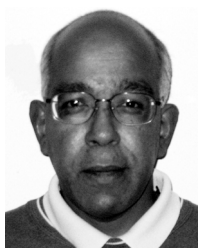

Ananthram Swami (SM'96) received the B.Tech. degree from the Indian Institute of Technolgoy, Mumbai, India, the M.S. degree from Rice University, Houston, and the Ph.D. degree from the University of Southern California (USC), San Diego, all in electrical engineering.

He has held positions with Unocal Corporation, USC, CS-3 and Malgudi Systems. He was a Statistical Consultant to the California Lottery, developed a Matlab-based toolbox for non-Gaussian signal processing, and has held visiting faculty positions at INP, Toulouse. He is currently with the US Army Research Laboratory where his work is in the broad area of signal processing, wireless communications and networking, including both sensor networks and MANETs.

Dr. Swami is chair of the IEEE Signal Processing Society's TC on Signal Processing for Communications, an Associate Editor of the IEEE TRANSACTIONS ON WIRELESS COMMUNICATIONS, and of the IEEE TRANSACTIONS ON SIGNAL PROCESSING. He has served as an Associate Editor of *IEEE Signal Processing Letters*, IEEE TRANSACTIONS ON CIRCUITS AND SYSTEMS—II: EXPRESS BRIEFS, and *IEEE Signal Processing Magazine*. He was co-organizer and co-chair of the 1993 IEEE-SPS HOS Workshop, the 1996 IEEE-SPS SSAP Workshop, and the 1999 ASA-IMA Workshop on Heavy-Tailed Phenomena. He was co-guest editor of a 2004 special issue (SI) of the IEEE Signal Processing Magazine (SPM) on "Signal Processing for Networking," a 2006 SPM SI on "Distributed signal processing in sensor networks," a 2006 EURASIP JASP SI on Reliable Communications over Rapidly Time-Varying Channels, and a 2006 EURASIP JWCN SI on "Wireless mobile ad hoc networks".